

The Challenge of Identifying the Origin of Black-Box Large Language Models

Ziqing Yang¹ Yixin Wu¹ Yun Shen² Wei Dai³ Michael Backes¹ Yang Zhang¹

¹CISPA Helmholtz Center for Information Security ²NetApp ³TikTok Inc.

Abstract

The tremendous commercial potential of large language models (LLMs) has heightened concerns about their unauthorized use. Third parties can customize LLMs through fine-tuning and offer only black-box API access, effectively concealing unauthorized usage and complicating external auditing processes. This practice not only exacerbates unfair competition, but also violates licensing agreements. In response, identifying the origin of black-box LLMs is an intrinsic solution to this issue. In this paper, we first reveal the limitations of state-of-the-art passive and proactive identification methods with experiments on 30 LLMs and two real-world black-box APIs. Then, we propose the proactive technique, PlugAE, which optimizes adversarial token embeddings in a continuous space and proactively plugs them into the LLM for tracing and identification. The experiments show that PlugAE can achieve substantial improvement in identifying fine-tuned derivatives. We further advocate for legal frameworks and regulations to better address the challenges posed by the unauthorized use of LLMs.¹

1 Introduction

Large language models (LLMs) have become integral parts of a wide range of services owing to their versatile capabilities in various domains. Facing the huge potential of LLMs, black-box LLM services [2, 9, 29, 31] that provide users only with API access are emerging as well as open-source LLMs [12, 19, 26, 36], fostering greater accessibility and transparency in the field. As shown in Table 1, we thoroughly reviewed the licenses of mainstream LLMs and LLM services from six organizations and observed that most organizations, such as OpenAI and Meta, prohibit third parties from rebranding their LLMs and impose restrictions on their commercial use. Despite these regulations, unofficial channels or unethical practices are dedicated to unauthorized releases of open-source models or leaks of proprietary black-box services [14, 20]. These actors may fine-tune these LLMs for specific tasks and provide black-box services without properly branding their model (see Figure 1). This violates the licensing agreements, exacerbates unfair competition, stifles innovation, and creates barriers to collaboration.

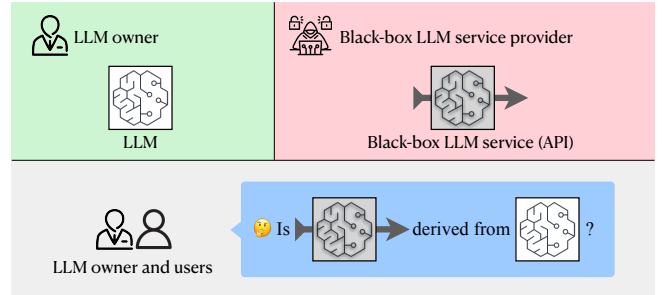


Figure 1: A black-box LLM identification scenario.

Identifying the origin of black-box LLMs is an intrinsic solution to the problem. In this work, we focus on the task of identifying the origin of a black-box LLM that might have been further fine-tuned on specific datasets. Specifically, given a *base* LLM, we aim to identify whether the black-box *suspect* models are its derivatives. We collect four LLMs as base models, and 30 LLMs and two LLM API services as suspect models for experiments. Existing identification methods can be categorized into two classes, i.e., *passive* and *proactive*, depending on whether the base LLM is proactively modified before release (see Figure 2 in the Appendix). Specifically, passive identification refers to methods that make identification without knowing whether the base model is modified or not [7, 14, 20, 25, 43]. Passive methods perform identification by querying with optimized text input, e.g., adversarial text, without making any changes to the model [14, 20]. Proactive methods modify the base models and identify the origins of suspect models based on the modifications [13, 22, 39, 40].

We first theoretically analyze the limitations of existing AE-based passive identification methods [14, 20] by formalizing them under a unified loss function. This framework reveals their dependence on discrete optimization, which impedes optimal solutions. We also observe that most existing proactive identification methods [6, 13, 22, 39, 40] fine-tune the LLM in a backdooring manner. This approach inevitably alters the model, disrupting its utility, and is computationally expensive. Moreover, it is prone to mitigation when the modified LLM undergoes further customization.

To overcome these challenges and better identify fine-tuned derivatives, we propose PlugAE, which proactively

¹We will release our code to facilitate research in the field.

Table 1: Usage scenarios by each organization’s model/API licenses. “-” denotes *not applicable*.

Usage Scenario	Organization					
	OpenAI [32]	Anthropic [3]	Google [11]	Mistral AI [28]	Meta [27]	Ai2 [1]
Open-Source Model ¹	✗	✗	✓	✓	✓	✓
Query-Only API Service	✓	✓	✓	✓	✗	✗
Fine-Tuning API Service	✓	✓	✓	✓	✗	✗
Commercial Use	✗	✗	-	✗	✓	✗
Commercial Use (Special Permission)	✓	-	✓	✓	✓	✓
Rebranding	✗	✗	✗	✗	✗	✗ ²

¹ The open-source models include licenses not yet approved by the Open Source Initiative (<https://opensource.org/license>).

² Note that Ai2’s OLMo series is under Apache 2.0 license [4] and allows rebranding, while there are other LLMs, such as tulu-2 series, are under the AI2 ImpACT License for Low Risk Artifacts (<https://huggingface.co/allenai/tulu-2-7b/blob/main/LICENSE.md>), which forbids rebranding.

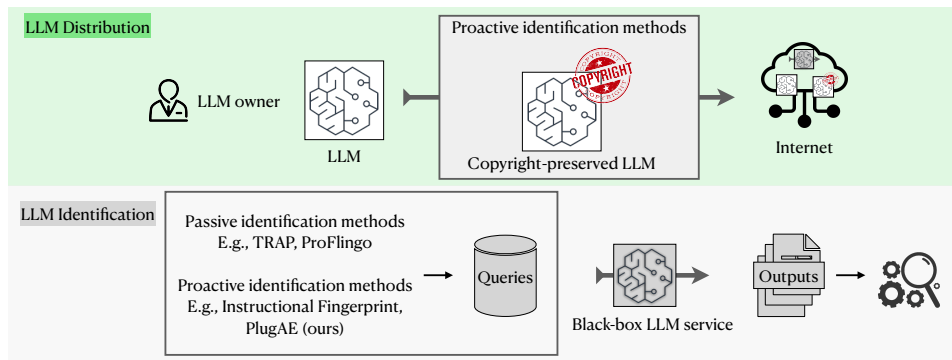


Figure 2: Passive and proactive methods to identify the origin of black-box LLMs.

modifies the base LLM by **plugging** in the **adversarial** token embeddings into the model without altering the model’s weights. Specifically, given a base model, `PlugAE` first optimizes a sequence of token embeddings as an adversarial example for a pre-defined query set, such as a set of question-answer pairs. `PlugAE` allows the model owner to define custom copyright tokens, each corresponding to an adversarial token embedding. Then, `PlugAE` plugs these token-embedding pairs into the LLM by adding the copyright tokens to the tokenizer’s vocabulary and injecting the token-embedding pairs into the model’s embedding layer. This process avoids modifying the model’s weights, ensuring that the model’s utility is preserved when the input does not include copyright tokens. We can later identify the suspect model by querying the suspect model with the query set and copyright tokens. We also provide theoretical evidence that `PlugAE` achieves performance closer to the optimal solution compared to existing AE-based methods. We further validate the theoretical findings by conducting extensive experiments on three base models and 32 suspect models, proving the effectiveness of `PlugAE` in practice.

Contributions. Overall, this study aims to ignite a crucial discussion on enhancing model transparency and accountability in an era defined by complex, often opaque, AI-driven interactions. Our contributions are as follows:

- We summarize the licenses and agreements of current

open-source LLMs and API services and raise the challenge of LLM identification.

- We evaluate both passive and proactive methods on the task of black-box LLM identification on various LLMs and show their unreliability on fine-tuned derivatives.
- We propose `PlugAE`, which proactively modifies the LLM by plugging the adversarial token embeddings into the model. We theoretically and empirically show its effectiveness and robustness in identifying fine-tuned derivatives.

2 Related Work

Existing black-box LLM identification methods can be categorized into two classes, i.e., *passive* and *proactive* identification, based on whether they require modifying the LLM *proactively* before distribution. We summarize the differences between the two types in [Table 2](#).

Passive Identification Methods. *Passive* LLM identification refers to the task that aims to identify the origin of an LLM [7, 14, 20, 25, 43] without requiring the model to be modified before release. For example, `TRAP` [14] and `ProFlingo` [20] are based on adversarial text prefix/suffix to query the LLM for target responses. Specifically, `TRAP` focuses on the black-box settings, while `ProFlingo` supports both black-box

Table 2: Different types of identification methods. “-” denotes *not applicable*. Note that “Modification?” denotes whether we will modify the model file, while “Change Weight?” represents whether the model’s weight would be changed.

Type	Method	Suspect Model	Base Model		
			Access	Modification?	Change Weight?
Passive	TRAP [14]	Black-Box	White-Box	-	-
	ProFLingo [20]	Black-Box	White-Box	-	-
Proactive	Instructional Fingerprint [39]	Black-Box	White-Box	✓	✓
	PlugAE	Black-Box	White-Box	✓	✗

and white-box scenarios. Some works [7, 25] analyze the LLM’s text or logits as fingerprints, focusing on their distribution and characteristics. However, such fingerprints are hard to maintain in derivatives of the LLM and may require white-box access. Besides, Zeng et al. [43] propose a human-readable fingerprint that encodes invariant terms in the model’s weight to a natural image under a white-box setting.

Proactive Identification Methods. One representative proactive identification method is LLM watermarking [6, 13, 22, 39, 40], most of which fine-tune the LLM in a backdooring way to enable traceability by the model owner. However, such watermarking that alters LLM parameters inevitably compromises model performance. Moreover, when the model owner seeks to further update or customize the model, the watermark may be lost during fine-tuning. In contrast, our proposed PlugAE preserves model integrity by avoiding parameter modifications. It demonstrates robustness even on fine-tuned LLMs. Reapplying PlugAE is also highly efficient, as it freezes the model entirely and only tunes adversarial embeddings, reducing trainable parameters from 7B to just 4K.

3 Problem Statement

LLM Licenses and Agreements. We summarize the types of services provided by the most mainstream LLMs on the market, along with their usage restrictions in Table 1. Among the six organizations we collected, OpenAI and Anthropic focus on providing API services, Meta and Ai2 release open-source models, while Google and Mistral AI have both API services and open-source models. We further analyze the usage restrictions in their licenses.

Our analysis reveals that many impose constraints on commercial use. Specifically, OpenAI requires businesses and developers that could benefit from their services to agree to further business terms [32, 34]. Anthropic stipulates that their services cannot be used for commercial or business purposes [3]. Mistral AI does not allow their services to be used for the benefit of a third party unless otherwise agreed in a separate contract with them [28]. Meta stipulates that if a third-party product or service exceeds 700 million monthly active users, they must apply for a special license from Meta; otherwise, they are not authorized to use Llama 2 [27]. Ai2 requires a third party to complete a derivative impact report with all model and data derivatives [1]. Moreover, none of these organizations permit third parties to rebrand their ser-

vices, such as by obscuring or removing copyright and trademark information.

Threat Model. Adversarial third parties may not possess the technology, computational resources, or sufficient time and funding. Thus, they intend to deliberately exploit LLMs without proper authorization, such as deploying unauthorized releases of open-source models or leaks of proprietary black-box services [14, 20]. The adversary can intentionally hide the copyright or trademark of the LLM and dishonestly claim that it is their own proprietary LLM. On the contrary, the defender can be the owner of an LLM or a third-party inspector ensuring the proper enforcement of intellectual property laws and regulations in the market. We term the LLM the defender obtains as a *base model* and the black-box LLM they want to identify as a *suspect model*. The defender aims to identify whether the suspect model is derived from the base model.

We argue that this identification task is non-trivial in reality. The defender often has white-box access to the base model and black-box access to the suspect model, as unauthorized services normally expose only black-box API to users. The adversary may align the base model with expected services by employing adapting techniques, for example, fine-tuning the base model on customized datasets and instructing it with specific system prompts. Such customization, while not intended, could help the adversary avoid identification by the defender. To further circumvent identification as the base model, the adversary may use specific prompts to respond to any queries about their true origin. They may also rebrand the LLM and rename the parameters. Additionally, they could rearrange the model’s weights, significantly changing the direction of parameter vectors without affecting the model’s performance [43].

4 PlugAE

We first analyze current AE-based passive identification methods both experimentally and theoretically. This allows us to conduct a comprehensive investigation of their inherent limitations and motivates our own method. Table 3 details the parameters, variables, and functions we use throughout the section.

4.1 Limitations of Existing Passive Identification Methods

Unified Loss. We present a unified loss function summarizing current AE-based identification methods [14, 20], as

Table 3: Notations.

m, n, k	Integers
x, y, a	Texts
$t_{1:n}$	Sequence of tokens
$\mathbf{e}_{1:n}$	Sequence of token embeddings
V	Set of all possible tokens
h	Prompt template
H	Set of prompt templates
\parallel	Text/Sequence concatenation
\circ	Function composition
$p_\phi(t_{n+1} \mathbf{e}_{1:n})$	Probability of the next token
$p_\theta(t_{n+1} t_{1:n})$	Probability of the next token
$I(s, s', z)$	Insert s' into s at position z
$\text{encode}(x)$	$= t_{1:n}^x, t_i^x \in V$
$\text{decode}(t)$	$= x^t$
$g(t_{1:n})$	$= \mathbf{e}_{1:n}, \mathbf{e}_i \in \mathbb{R}^d$
$p_\phi(t_{n+1} \mathbf{e}_{1:n})$	$= g \circ p_\theta(t_{n+1} t_{1:n})$
$p_\phi(t_{n+1:n+m} \mathbf{e}_{1:n})$	$= \prod_{i=1}^m p_\phi(t_{n+i} \mathbf{e}_{1:n+i-1})$
$\mathcal{L}^e(t_{n+1:n+m}, \mathbf{e}_{1:n})$	$= -\log p_\phi(t_{n+1:n+m} \mathbf{e}_{1:n})$
$p_\theta(t_{n+1:n+m} t_{1:n})$	$= \prod_{i=1}^m p_\theta(t_{n+i} t_{1:n+i-1})$
$\mathcal{L}(t_{n+1:n+m}, t_{1:n})$	$= -\log p_\theta(t_{n+1:n+m} t_{1:n})$

introduced in [Appendix A.1](#):

$$\mathcal{L}_{\text{AE}}(y^*, x, a) = \sum_{h \in H} \mathcal{L}(t^{y^*}, I(t^{h(x)}, t^a, z_h)), \quad (1)$$

where $I(t^{h(x)}, t^a, z_h)$ denotes the insertion of the token sequence t^a into the token sequence $t^{h(x)}$ of the input x , at the position specified by z_h . It is important to note that the position z_h is adaptable, enabling support for various prompt templates. For instance, the unified loss \mathcal{L}_{AE} can be translated into $\mathcal{L}_{\text{ProFlingo}}$ if we insert the adversarial example a as input x 's prefix, i.e., let $I(t^{h(x)}, t^a, z_h) := t^{h(a||x)}, \forall h \in H$. It is also noteworthy that the insertion operation $I(\cdot, \cdot, \cdot)$ can be applied not only to token sequences but also to embedding sequences, thereby extending its applicability across different levels of representation.

Limitations of TRAP and ProFlingo. We experiment on the effectiveness and the efficiency of TRAP [14] and ProFlingo [20] in [Appendix A](#) and compare them under the unified loss \mathcal{L}_{AE} . As discussed above, the unified loss can be translated into the $\mathcal{L}_{\text{ProFlingo}}$ loss function when $I(t^{h(x)}, t^a, z_h) := t^{h(a||x)}$. Likewise, this unified loss can be adapted to $\mathcal{L}_{\text{TRAP}}$ by defining the prompt template collection as $H = \{h\}$, where h represents the default template of the base model, and appending a after x , i.e., setting $I(t^{h(x)}, t^a, z_h) := t^{h(x||a)}$. We find $\mathcal{L}_{\text{TRAP}}$ is more restricted as it optimizes to only one prompt template, while $\mathcal{L}_{\text{ProFlingo}}$ optimizes several prompt templates simultaneously (see [Equation 10](#)), which allows a more generalizable adversarial text that is resilient to larger disturbances. This could explain why TRAP can only identify the base model itself, while ProFlingo can identify more derivatives of the base model, as shown in [Appendix A.3](#).

Recall that we focus on the task of black-box LLM identification, where interaction with the target model is restricted

to text inputs. The defender optimizes an adversarial prefix/suffix to query the suspect model. However, because text is composed of discrete tokens, the optimization process inherently operates in a discrete space. For example, ProFlingo first calculates the gradient for each token t_i^a in the prefix a in each epoch as $\nabla_{t_i^a} \mathcal{L}_{\text{AE}}$. As we can only replace t_i^a instead of optimizing it directly, ProFlingo updates the adversarial prefix by replacing multiple tokens in each epoch. Based on the top- k tokens with the most negative gradients, a set of candidate tokens for replacement is sampled. Subsequently, the loss associated with each potential replacement token is computed. The token with the minimal loss is then selected. TRAP follows a similar process, optimizing over a discrete set of inputs. However, such discrete optimization approaches present significant challenges. Given the limited number of tokens and the computationally intensive nature of the optimization process, it is difficult to achieve a local optimum by design.

4.2 Method

Overview. Our evaluation thus far shows that existing passive and proactive approaches are unreliable for identifying the fine-tuned derivatives of the base LLM. To address this limitation, we propose PlugAE, an efficient and effective plug-in model watermarking method that combines the advantages of both passive and proactive methods. PlugAE is also based on adversarial examples. Different from existing methods, PlugAE shifts the optimization focus from discrete tokens to continuous token embeddings. PlugAE allows the user to set a copyright token that corresponds to the optimized token embedding and plugs this token-embedding pair into the model as a watermark. This process requires editing the model's tokenizer and the corresponding embedding layer that transforms encoded tokens into token embeddings. Unlike existing model watermarking methods such as Instructional Fingerprint, PlugAE does not need to change the model's weights, thus, the utility is well-preserved. By concentrating on token embeddings rather than discrete tokens, PlugAE makes the optimization continuous, which in turn leads to improved performance and stability in AE-based techniques.

Method. Formally, we aim to optimize a sequence of adversarial token embeddings $\mathbf{e}_{1:k}^a$ to minimize the following loss function:

$$\begin{aligned} \mathcal{L}_{\text{PlugAE}}^e(y^*, x, \mathbf{e}_{1:k}^a) &= \sum_{h \in H} \mathcal{L}^e(t^{y^*}, I(g(t^{h(x)}), \mathbf{e}_{1:k}^a, z_h)) \\ &= \sum_{h \in H} \mathcal{L}^e(t^{y^*}, I(\mathbf{e}^{h(x)}, \mathbf{e}_{1:k}^a, z_h)), \end{aligned} \quad (2)$$

where k is the number of token embeddings and $\mathbf{e}^{h(x)}$ denotes the sequence of the encoded token embeddings of the prompted input $h(x)$. $I(\mathbf{e}^{h(x)}, \mathbf{e}_{1:k}^a, z_h)$ represents inserting the adversarial embeddings $\mathbf{e}_{1:k}^a$ into the input token embedding sequence $\mathbf{e}^{h(x)}$ at position z_h . Overall, we optimize the adversarial embeddings $\mathbf{e}_{1:k}^a$ to minimize the loss $\mathcal{L}_{\text{PlugAE}}^e$:

$$\arg \min_{\mathbf{e}_{1:k}^a} \mathcal{L}_{\text{PlugAE}}^e(y^*, x, \mathbf{e}_{1:k}^a). \quad (3)$$

After we obtain the optimized adversarial token embeddings $\mathbf{e}_{1:k}^a$, we can define copyright token that corresponds to each adversarial embedding and plug them in the model as a watermark. Specifically, we add the copyright tokens in the vocabulary of the model’s tokenizer and insert the corresponding copyright token-embedding pair into the model file. Note that this process does not modify the model’s parameters. In this sense, when the model owner wants to identify whether the origin of a black-box LLM is their model, they can query the model with copyright tokens and the corresponding questions and check whether the model responds with target outputs.

Reaching the Optimal of AE-Based Methods. Based on the loss function of our `PlugAE` and the unified loss provided in [Section 4.1](#), we theoretically prove that `PlugAE` can reach the optimal of AE-based methods by analyzing the optimal loss.

Hypothesis 4.1. For most LLMs, we assume their embedding layer $g : V^n \rightarrow \mathbb{R}^{d \times n}$ is injective, where d is the dimension of the token embedding and n is the length of the token sequence.

In practice, token embeddings in LLMs are often represented as d -dimensional vectors. Consequently, the size of the vocabulary V is much smaller than the dimensionality d of the embedding space, i.e., $|V| \ll |\mathbb{R}^d|$. Such a high dimensionality increases the likelihood that different tokens will have distinct embeddings, thereby making g more likely to be injective. To empirically verify this hypothesis, we experiment with our four base LLMs and the other 18 LLMs. Specifically, for each LLM, we calculate the cosine similarity between every pair of token embeddings. We considered two embeddings to be similar if their cosine similarity exceeded 0.99. The results of our experiments demonstrate that, across all the LLMs tested, the token embeddings were pairwise distinct. The empirical evidence supports that our [Claim 4.1](#) holds for most LLMs in practice.

Lemma 4.2. Based on [Claim 4.1](#), the inverse function q of the embedding layer g is non-differentiable.

Proof. Let g be the mapping from tokens to embeddings, and let q be its inverse, defined as:

$$q : \mathbb{R}^{d \times n} \rightarrow V^n, \quad (4)$$

where d is the dimension of the token embedding, and n is the length of the embedding sequence. Note that V is a discrete space, which contains pre-defined tokens that are discontinuous. Thus, q is non-differentiable due to the discrete nature of its output. \square

Lemma 4.3. Based on [Claim 4.1](#), the unified loss \mathcal{L}_{AE} is derived from `PlugAE`’s loss $\mathcal{L}_{\text{PlugAE}}^e$ with the application of the inverse function q .

Proof. Firstly, we prove $q \circ \mathcal{L}^e(t_{n+1:n+m}, \mathbf{e}_{1:n}) = \mathcal{L}(t_{n+1:n+m}, t_{1:n}^e)$. Based on [Equation 4](#), q maps a token embedding sequence to a discrete token sequence. Thus, $q \circ \mathcal{L}^e(\cdot)$ is a transformation of input domains from $\mathbb{R}^{d \times n}$

to V^n . As $p_\phi(t_{n+1} | \mathbf{e}_{1:n}) = g \circ p_\theta(t_{n+1} | t_{1:n})$, we can infer $q \circ p_\phi(t_{n+1} | \mathbf{e}_{1:n}) = q \circ g \circ p_\theta(t_{n+1} | t_{1:n}) = p_\theta(t_{n+1} | t_{1:n})$.

$$\begin{aligned} q \circ \mathcal{L}^e(t_{n+1:n+m}, \mathbf{e}_{1:n}) &= q \circ -\log p_\phi(t_{n+1:n+m} | \mathbf{e}_{1:n}) \\ &= q \circ -\sum_{i=1}^m \log p_\phi(t_{n+i} | \mathbf{e}_{1:n+i-1}) \\ &= -\sum_{i=1}^m q \circ \log p_\phi(t_{n+i} | \mathbf{e}_{1:n+i-1}) \\ &= -\sum_{i=1}^m \log p_\theta(t_{n+i} | t_{1:n+i-1}^e) \\ &= -\log \prod_{i=1}^m p_\theta(t_{n+i} | t_{1:n+i-1}^e) \\ &= -\log p_\theta(t_{n+1:n+m} | t_{1:n}^e) \\ &= \mathcal{L}(t_{n+1:n+m}, t_{1:n}^e). \end{aligned} \quad (5)$$

We conclude $q \circ \mathcal{L}^e(t_{n+1:n+m}, \mathbf{e}_{1:n}) = \mathcal{L}(t_{n+1:n+m}, t_{1:n}^e)$.

Then, we prove $q(I(\mathbf{e}_{1:n}, \mathbf{e}'_{1:m}, z)) = I(q(\mathbf{e}_{1:n}), q(\mathbf{e}'_{1:m}), z)$. Let z be the k -th position of $\mathbf{e}_{1:n}$, $k \in [0, n]$, $s_{1:0}$ and $s_{n+1:n}$ denote a null sequence.

From left:

$$\begin{aligned} q(I(\mathbf{e}_{1:n}, \mathbf{e}'_{1:m}, z)) &= q(\{\mathbf{e}_{1:k}, \mathbf{e}'_{1:m}, \mathbf{e}_{k+1:n}\}) \\ &= t^{\{\mathbf{e}_{1:k}, \mathbf{e}'_{1:m}, \mathbf{e}_{k+1:n}\}} \\ &= \{t_{1:k}^e, t_{1:m}^e, t_{k+1:n}^e\}. \end{aligned} \quad (6)$$

For the right side:

$$\begin{aligned} I(q(\mathbf{e}_{1:n}), q(\mathbf{e}'_{1:m}), z) &= I(t_{1:n}^e, t_{1:m}^e, z) \\ &= \{t_{1:k}^e, t_{1:m}^e, t_{k+1:n}^e\}. \end{aligned} \quad (7)$$

Thus, we conclude $q(I(\mathbf{e}_{1:n}, \mathbf{e}'_{1:m}, z)) = I(q(\mathbf{e}_{1:n}), q(\mathbf{e}'_{1:m}), z)$. Finally, we have:

$$\begin{aligned} q \circ \mathcal{L}_{\text{PlugAE}}^e(y^*, x, \mathbf{e}_{1:m}^a) &= q \circ \sum_{h \in H} \mathcal{L}^e(t^{y^*}, I(\mathbf{e}^{h(x)}, \mathbf{e}_{1:m}^a, z_h)) \\ &= \sum_{h \in H} \mathcal{L}(t^{y^*}, q(I(\mathbf{e}^{h(x)}, \mathbf{e}_{1:m}^a, z_h))) \\ &= \sum_{h \in H} \mathcal{L}(t^{y^*}, I(q(\mathbf{e}^{h(x)}), q(\mathbf{e}_{1:m}^a), z_h)) \\ &= \sum_{h \in H} \mathcal{L}(t^{y^*}, I(t^{h(x)}, t_{1:m}^a, z_h)) \\ &= \mathcal{L}_{AE}(y^*, x, a). \end{aligned} \quad (8)$$

\square

Lemma 4.4. Given q is non-differentiable ([Claim 4.2](#)), $\mathcal{L}_{\text{PlugAE}}^e$ can reach closer or equal to the optimal solution compared to the unified loss \mathcal{L}_{AE} .

Proof. Based on [Claim 4.3](#), $\mathcal{L}_{AE} = q \circ \mathcal{L}_{\text{PlugAE}}^e$. The non-differentiability of q introduces points in the loss landscape where gradients are either undefined or lead to instability. This can cause optimization algorithms, particularly those

Table 4: Performance of proactive identification methods on CSN-tuned Models.

Model Version	Method	llama-7b	Llama-2-7b	Mistral-7B-v0.1
Original	Instructional Fingerprint	0.00	0.00	0.00
	PlugAE	0.00	0.00	0.00
Post-Proactive	Instructional Fingerprint	1.00	1.00	1.00
	PlugAE	1.00	1.00	1.00
CSN-Tuned	Instructional Fingerprint	0.00	0.88	0.25
	PlugAE	0.98	0.98	0.78

relying on gradient descent, to struggle with convergence, potentially getting stuck in flat regions or diverging near discontinuities. On the other hand, $\mathcal{L}_{\text{PlugAE}}^e$, provides a smooth loss landscape. Gradient-based methods can reliably compute gradients and update parameters effectively, allowing for consistent progress toward the optimal solution. Thus, $\mathcal{L}_{\text{PlugAE}}^e$ is more likely to reach closer or equal to the optimal solution compared to \mathcal{L}_{AE} , which is hindered by the non-differentiable function q . \square

Claim 4.5. *Based on Claim 4.4, the optimization of our PlugAE can be closer to the optimal compared with current AE-based methods that adopt the unified loss \mathcal{L}_{AE} .*

Claim 4.5 shows that our PlugAE can explore the extent of existing passive identification methods.

Comparison With Existing Proactive Methods. Proactive methods allow model owners to proactively protect their intellectual property before model distribution. Existing methods, known as model watermarking, fine-tune the LLM to learn a watermark pattern. Our PlugAE differs from these methods in the following two aspects. Firstly, our PlugAE does not require modifying the model’s weight, thus preserving the model’s utility. This is different from model watermarking, which requires updating the model’s parameters to learn the watermark pattern. The second aspect is that we allow the model owner to define the copyright tokens. This not only reduces the collision of copyright tokens for different models using our PlugAE, but also provides chances that the corresponding adversarial token embeddings could remain after further fine-tuning.

Summary. Our PlugAE utilizes the advantage of adversarial examples and proactively modifies the model before distribution to help identification. We theoretically prove that PlugAE could be more optimal compared with current AE-based identification methods. We will further conduct experiments to show the effectiveness of our PlugAE.

4.3 Experimental Settings

Models. We utilize three *base models*, including llama-7b [36], Llama-2-7b [37], and Mistral-7B-v0.1 [19]. We have white-box access to them and aim to identify whether they are the origin of the suspect black-box LLM. Then, we collect extensive models as *suspect models* for evaluation, including 30 open-source LLMs and two real-world black-box APIs. Specifically, some models derived from

the base models are released officially, e.g., Llama-2-7b-chat [37] developed by Meta. Some are released by other institutes, e.g., vicuna-7b-v1.3 [24] (fine-tuned on llama-7b) from LMSYS Org and tulu-2-7b [18] (fine-tuned on Llama-2-7b) from AllenAI. We also collect other model families, such as OLMo [12]. As for the two black-box APIs, we collect gpt-4-turbo-2024-04-09 [33] and claude-3-5-sonnet-20240620 [2] as suspect models for evaluation.

Investigation Setup. In the experiments, we place the adversarial embeddings as the prefix of the input query x ’s embedding sequence \mathbf{e}^x following ProFlingo. We utilize llama-7b, Llama-2-7b, and Mistral-7B-v0.1 as our base models. We follow the query set of ProFlingo. We set the number of adversarial token embeddings as 1 and set the copyright token with a randomly generated 5-digit string “mkahg.” We optimize a universal adversarial token embedding for all queries. We set the learning rate to 0.1 with the Adam optimizer and run 30 epochs for each sample.

Customization. For fine-tuning, we use CodeSearchNet (CSN) [17], a widely used dataset that contains about six million functions from open-source code spanning six programming languages (Go, Java, JavaScript, PHP, Python, and Ruby) for customization. We adhere to the training parameters of Alpaca [35] and fine-tune the watermarked models for 15,000 steps on four NVIDIA A100 GPUs with 40 GB of memory. Then, we evaluate the utility of the customized models on HellaSwag [42] and MMLU [16] under the zero-shot setting.

Evaluation Metric. We use the target response rate (TRR) as our evaluation metric, which measures the ratio of the number of queries that the suspect model outputs the target output over the number of all queries. A higher TRR indicates a higher probability that the suspect model is derived from the base model.

Baselines. We take Instructional Fingerprint [39] as the baseline of proactive methods, which is a state-of-the-art model watermarking method for LLMs.

4.4 Experimental Results

Effectiveness. Experimental results of our PlugAE depicted in Table 4 show the effectiveness in identifying and robustness against fine-tuning. We observe that both PlugAE and Instructional Fingerprint achieve a TRR of 1.00 when we identify the suspect model without further fine-tuning. After fine-tuning on CSN, PlugAE maintains a high TRR of 0.98 on both fine-tuned llama-7b and Llama-2-7b mod-

Table 5: Utility on HellaSwag and MMLU. [Method]-CSN denotes that the model is first proactively modified by [Method] and then fine-tuned on CSN.

Dataset	Model	Original	PlugAE	IF	PlugAE-CSN	IF-CSN
HellaSwag	llama-7b	0.57±0.005	0.57±0.005	0.57±0.005	0.57±0.005	0.57±0.005
	Llama-2-7b	0.57±0.005	0.57±0.005	0.58±0.005	0.58±0.005	0.58±0.005
	Mistral-7B-v0.1	0.61±0.005	0.61±0.005	0.61±0.005	0.60±0.005	0.60±0.005
MMLU	llama-7b	0.32±0.059	0.32±0.059	0.31±0.057	0.32±0.059	0.33±0.059
	Llama-2-7b	0.41±0.088	0.41±0.088	0.41±0.089	0.40±0.085	0.42±0.085
	Mistral-7B-v0.1	0.60±0.133	0.60±0.133	0.60±0.135	0.57±0.126	0.59±0.115

Table 6: Performance of our PlugAE. “Non-derivative Models” represent the other suspect models, including the black-box APIs. We observe that the TRRs for all non-derivative models are 0.00. This is because those models do not contain the corresponding copyright tokens or the adversarial embeddings. They will not respond with target answers when querying with copyright tokens.

Suspect Model	Base Model		
	llama-7b	Llama-2-7b	Mistral-7B-v0.1
yahma/llama-7b-hf	1.00	0.00	0.00
lmsys/vicuna-7b-v1.3	0.68	0.00	0.00
TheBloke/guanaco-7B-HF	0.78	0.00	0.00
meta-llama/Llama-2-7b-hf	0.00	1.00	0.00
meta-llama/Llama-2-7b-chat-hf	0.00	0.36	0.00
lmsys/vicuna-7b-v1.5	0.00	0.24	0.00
codellama/CodeLlama-7b-hf	0.00	0.00	0.00
codellama/CodeLlama-7b-Python-hf	0.00	0.00	0.00
codellama/CodeLlama-7b-Instruct-hf	0.00	0.06	0.00
allenai/tulu-2-7b	0.00	0.64	0.00
allenai/tulu-2-dpo-7b	0.00	0.58	0.00
allenai/scitulu-7b	0.00	0.50	0.00
microsoft/Orca-2-7b	0.00	0.24	0.00
georgesung/llama2_7b_chat_uncensored	0.00	0.94	0.00
mistralai/Mistral-7B-v0.1	0.00	0.00	1.00
mistralai/Mistral-7B-Instruct-v0.1	0.00	0.00	0.14
HuggingFaceH4/zephyr-7b-beta	0.00	0.00	0.76
mistralai/Mistral-7B-v0.3	0.00	0.00	0.90
mistralai/Mistral-7B-Instruct-v0.3	0.00	0.00	0.78
Non-derivative Models	0.00	0.00	0.00

els, which outperforms Instructional Fingerprint by 0.98 and 0.10, respectively. This indicates that the performance of fine-tuning-based model watermarking relies on the customization dataset and shows that our proactive identification method is more robust against fine-tuning compared with model watermarking.

We further evaluate the utility of these models, including the original LLMs, the LLM after modification, and the modified LLM after customization. Results shown in Table 5 indicate that the utility maintains being watermarked by Instructional Fingerprint or after fine-tuning on CSN. Although Instructional Fingerprint does not affect the utility much, our PlugAE achieves the same performance as the original model under the same random seed. This makes sense as we do not need to modify the model’s parameters.

A Broader Evaluation. To broaden our evaluation under a real-world setting, we further evaluate PlugAE on our suspect models. However, it is challenging for us to fine-tune

the LLMs with PlugAE in real-world settings. Then, we simulate the fine-tuned models by plugging the copyright token of the base model into their real-world derivatives. For example, we add the copyright token of Llama-2-7b into meta-llama/Llama-2-7b-chat-hf, lmsys/vicuna-7b-v1.5, and the other eight derivatives.

This is practical as the token embedding of copyright token is hard to modify during fine-tuning. This is because we assume the copyright token is defined by the model owner and is hard to guess. In this sense, the copyright token should rarely appear in the training corpus of the fine-tuning dataset, which is composed of natural language, and thus this will not be affected by the backpropagation in the fine-tuning process. We empirically verify this by comparing the cosine similarity between the embedding of copyright token in the model before and after fine-tuning. Results show that the copyright token’s embedding remains exactly the same after fine-tuning in all three base models, i.e., all cosine similarities are 1.00.

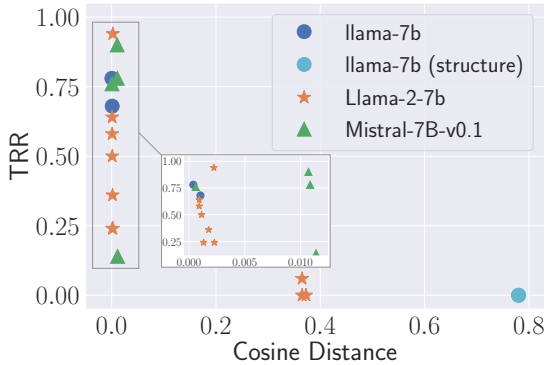


Figure 3: Relationship between TRRs and the model weights’ cosine distance with the base model. The inner is a zoomed-in subgraph focusing on the region that excludes counterexamples, offering a more fine-grained view. This reveals a negative correlation between TRRs and cosine distances, suggesting that larger cosine distances are associated with lower TRRs.

Experimental results of our PlugAE are depicted in Table 6. We observe that, given a base model with PlugAE, the TRRs of suspect models that are non-derivative are 0.00. This is because those models do not have the corresponding copyright token or the adversarial embeddings. In this sense, when we query the model with copyright tokens, non-derivative models would not respond with the target answer. For derivatives, TRRs are generally high. For example, taking llama-7b as the base model, the TRR of the related suspect model TheBloke/guanaco-7B-HF is 0.78. Based on Llama-2-7b, the TRR of georgesung/llama2-7b chat uncensored is 0.94, while the TRR of allenai/tulu-2-7b is 0.64. Based on Mistral-7B-v0.1, the TRR of HuggingFaceH4/zephyr-7b-beta is 0.76, and the TRR of mistralai/Mistral-7B-Instruct-v0.3 is 0.78. This indicates that the derivatives tend to respond with target answers when querying with copyright tokens, while the unrelated models fail. Our PlugAE illustrates more confidence in distinguishing between related and unrelated suspect models.

Counterexamples Analysis. However, there are still some counterexamples. Based on Llama-2-7b, the TRRs of codellama/CodeLlama-7b-hf and codellama/CodeLlama-7b-Python-hf are 0.00, while the TRR of codellama/CodeLlama-7b-Instruct-hf is 0.06. Thus, we further examined the reason why PlugAE performs worse on these models. Specifically, we measure the difference between the base model and its derivatives. We compute the cosine distance between the weights of the two models. Figure 3 shows the relationship between the TRRs and the cosine distance between the related suspect models and the base model. A large cosine distance indicates a large weight shift from the base model. The deviant points show that if the weight of the derivative is too distant from the base model, the performance of PlugAE would drop drastically. For example, the cosine distance between codellama/CodeLlama-7b-hf and Llama-2-7b reaches 0.3653, which is much higher than other Llama-2-7b’s derivatives, e.g., allenai/tulu-2-7b (0.0009). PlugAE only achieves a TRR of 0.00 on codellama/CodeLlama-7b-hf while reaching a TRR of 0.64 on allenai/tulu-2-7b. This

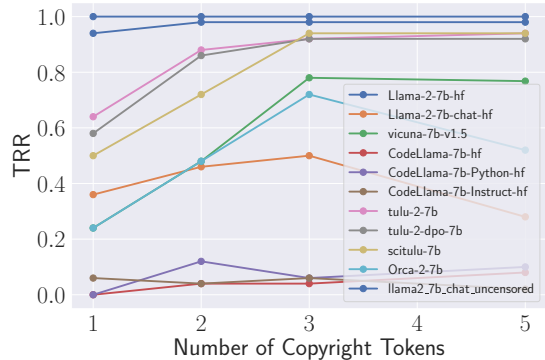


Figure 4: Influence of the number of tokens on Llama-2-7b.

suggests that PlugAE could be dodged when there is a significant weight shift from the base model.

Additionally, openlm-research/open_llama_7b presents a permissively licensed open-source reproduction of Meta AI’s llama-7b model, i.e., it uses llama-7b’s structure and is trained on another dataset by another organization. We compute the cosine distance between it and its derivatives with llama-7b as well and label them as llama-7b (structure). Results in Figure 3 show that their weights are more distant from llama-7b, and PlugAE failed to identify them with llama-7b. This provides a new scenario where the adversary steals the architecture of an LLM illicitly, trains it from scratch, and distributes it for unauthorized use, e.g., commercial purposes. We do not include the discussion on this topic and leave it as future work.

The inner figure in Figure 3 excludes those deviant points and zooms in. The figure indicates a negative correlation between TRRs and cosine distances, suggesting that larger cosine distances are associated with lower TRRs. Take Llama-2-7b as the base model, for instance. PlugAE achieves a TRR of 0.64 on allenai/tulu-2-7b, while its cosine distance with Llama-2-7b is only 0.0009. If the weight of the derivative is more distant from the base model, the performance of PlugAE would drop. For instance, the TRR on microsoft/Orca-2-7b is 0.24, with a cosine distance of 0.0023.

4.5 Ablation Study

Influence of Different Copyright Tokens. In the main experiments, we conduct PlugAE using a randomly generated 5-digit string as the copyright token. To investigate the influence of different copyright token choices, we experiment with the other two different copyright tokens. The first is that we use a popular random password generator² to generate a 20-digit length password as the copyright token, i.e., “c*zNFj.7}4E5~hHAq9Nh.” The other is “cf,” which exists in the Mistral-7b’s default vocabulary but not in llama-7b or Llama-2-7b’s vocabulary. In the experiments, we got the same results using different copyright tokens. This is intuitive, as different copyright tokens correspond to the same token embedding.

Influence of Different Numbers of Tokens. To investigate

²<https://1password.com/password-generator>.

the influence of the number of copyright tokens, we further experiment with the number of tokens of 2, 3, and 5 on the Llama-2-7b model. For copyright token selection, we randomly generate a 5-digit string for each token embedding. Results in Figure 4 show that a larger token number could achieve a better TRR on the derivatives. For instance, the TRR on allenai/scitulu-7b increases from 0.50 to 0.94 when the token number increases to 5. However, when the token number is too large, i.e., 5, the TRRs on the derivatives would even drop. For example, the TRR on microsoft/Orca-2-7b drops to 0.52 when the token number is 5, while it is 0.72 when the token number is 3. Note that the TRRs for non-derivatives remain to be 0.

5 Our Vision

As we delve deeper into methods for identifying black-box LLMs (see Appendix B), there is still much to be done to safeguard the intellectual property rights of developers and owners of LLMs, as well as other foundation models [5, 23, 38, 41]. To begin with, we present a real example of two large vision-language models (VLMs) as an introduction. In June 2024, a user on GitHub raised concerns that the Llama3-V model may have improperly copied elements from the MiniCPM-Llama3-V 2.5 project [41], prompting a thorough investigation by the authors of the accused model.³ The inquiry revealed striking similarities in code structure and minor variable name changes between Llama3-V and MiniCPM-Llama3-V 2.5. Further similarities were found in behavior, particularly in specialized tasks such as recognizing Tsinghua Bamboo Characters, which were from the in-house training data of MiniCPM-Llama3-V 2.5. This serves as a clear indicator of the infringement and exemplifies the potential benefits of proactive identification strategies.

Beyond technological solutions, we emphasize the importance of nurturing a robust open-source community. Such communities not only serve as guardians preventing the unauthorized use of copyrighted material but also as incubators for technological innovation. The incident with Llama3-V highlights the pivotal role that the community can play in uncovering and addressing infringement. Moreover, by participating in open-source projects, researchers and developers gain access to a collaborative environment where they can innovate and refine technologies at a pace that individual efforts cannot match.

Furthermore, while current licensing practices for foundation models are extensive (see Table 1), there is a notable deficiency in the regulation of the training data used to develop these models. The vast corpora required to train such models are often neither open-sourced nor clearly documented [19, 30, 36], raising significant concerns about copyright compliance and transparency. This lack of oversight and regulation can lead to ambiguities in ownership and ethical use, which are crucial for maintaining trust and integrity within the AI community. To address these challenges, we advocate for clearer legislation and more stringent regulatory frameworks that not only keep pace with technological ad-

vancements but also ensure that the copyrights of large training datasets are adequately protected [8].

6 Conclusion

In this paper, we focus on the task of black-box LLM identification. We evaluate both passive and proactive identification methods on various LLMs and showcase their unreliability against fine-tuning. Our theoretical analysis shows that existing AE-based methods are hard to reach the optimal for their discrete optimization process. Thus, we propose PlugAE, a proactive identification method that plugs the adversarial token embeddings into the LLM. Experiments show our effectiveness even in identifying the fine-tuned derivatives. Further, we summarize current challenges and share our vision on LLM-related copyright protection issues, covering technology, law, and public ethics.

Impact Statement

By raising awareness of the risks of the unauthorized use of LLMs, our work aims to contribute to developing a more robust and secure open-source environment and urges for a more reliable way to identify LLMs. With theoretical analysis, we explore the inner limitations of current AE-based passive identification methods and provide an alternative way to overcome such limitations. We believe our work can motivate more advanced identification methods in this field. Last but not least, all LLMs used in our research are publicly available. We do not use any unauthorized LLMs in our study, thereby adhering to ethical standards and legal compliance.

References

- [1] Allen AI. Ai2 impact license for low risk artifacts. <https://huggingface.co/allenai/tulu-2-7b/blob/main/LICENSE.md>. 2, 3
- [2] Anthropic. Claude. <https://claude.ai/>. 1, 6, 12
- [3] Anthropic. Consumer terms of service. <https://www.anthropic.com/legal/consumer-terms>. 2, 3
- [4] Apache. Apache license version 2.0. <https://www.apache.org/licenses/LICENSE-2.0>. 2
- [5] Lin Chen, Jinsong Li, Xiaoyi Dong, Pan Zhang, Conghui He, Jiaqi Wang, Feng Zhao, and Dahua Lin. ShareGPT4V: Improving Large Multi-Modal Models with Better Captions. *CoRR abs/2311.12793*, 2023. 9
- [6] Miranda Christ, Sam Gunn, Tal Malkin, and Mariana Raykova. Provably Robust Watermarks for Open-Source Language Models. *IACR Cryptology ePrint Archive*, 2024. 1, 3
- [7] Nirav Diwan, Tanmoy Chakraborty, and Zubair Shafiq. Fingerprinting Fine-tuned Language Models in the Wild. In *Annual Meeting of the Association for Computational Linguistics and International Joint Conference on Natural Language Processing (ACL/IJCNLP)*, pages 4652–4664. ACL, 2021. 1, 2, 3

³<https://github.com/OpenBMB/MiniCPM-V/issues/196>.

- [8] European Commission. Ei ai act. <https://eurlex.europa.eu/eli/reg/2024/1689>. 9
- [9] GitHub. Copilot. <https://github.com/features/copilot>. 1
- [10] Ian Goodfellow, Jonathon Shlens, and Christian Szegedy. Explaining and Harnessing Adversarial Examples. In *International Conference on Learning Representations (ICLR)*, 2015. 11
- [11] Google. Gemini api additional terms of service. <https://ai.google.dev/gemini-api/terms>. 2
- [12] Dirk Groeneveld, Iz Beltagy, Pete Walsh, Akshita Bhagia, Rodney Kinney, Oyvind Tafjord, Ananya Harsh Jha, Hamish Ivison, Ian Magnusson, Yizhong Wang, Shane Arora, David Atkinson, Russell Authur, Khyathi Raghavi Chandu, Arman Cohan, Jennifer Dumas, Yanai Elazar, Yuling Gu, Jack Hessel, Tushar Khot, William Merrill, Jacob Morrison, Niklas Muenighoff, Aakanksha Naik, Crystal Nam, Matthew E. Peters, Valentina Pyatkin, Abhilasha Ravichander, Dustin Schwenk, Saurabh Shah, Will Smith, Emma Strubell, Nishant Subramani, Mitchell Wortsman, Pradeep Dasigi, Nathan Lambert, Kyle Richardson, Luke Zettlemoyer, Jesse Dodge, Kyle Lo, Luca Soldaini, Noah A. Smith, and Hannaneh Hajishirzi. OLMo: Accelerating the Science of Language Models. *CoRR abs/2402.00838*, 2024. 1, 6, 12
- [13] Chenxi Gu, Chengsong Huang, Xiaoqing Zheng, Kai-Wei Chang, and Cho-Jui Hsieh. Watermarking Pre-trained Language Models with Backdooring. *CoRR abs/2210.07543*, 2022. 1, 3
- [14] Martin Gubri, Dennis Ulmer, Hwaran Lee, Sangdoon Yun, and Seong Joon Oh. TRAP: Targeted Random Adversarial Prompt HoneyPot for Black-Box Identification. In *Annual Meeting of the Association for Computational Linguistics (ACL)*. ACL, 2024. 1, 2, 3, 4, 11, 12, 15
- [15] Chuan Guo, Alexandre Sablayrolles, Hervé Jégou, and Douwe Kiela. Gradient-based Adversarial Attacks against Text Transformers. In *Conference on Empirical Methods in Natural Language Processing (EMNLP)*, pages 5747–5757. ACL, 2021. 11
- [16] Dan Hendrycks, Collin Burns, Steven Basart, Andy Zou, Mantas Mazeika, Dawn Song, and Jacob Steinhardt. Measuring Massive Multitask Language Understanding. In *International Conference on Learning Representations (ICLR)*, 2021. 6
- [17] Hamel Husain, Ho-Hsiang Wu, Tiferet Gazit, Miltiadis Allamanis, and Marc Brockschmidt. CodeSearchNet Challenge: Evaluating the State of Semantic Code Search. *CoRR abs/1909.09436*, 2019. 6
- [18] Hamish Ivison, Yizhong Wang, Valentina Pyatkin, Nathan Lambert, Matthew E. Peters, Pradeep Dasigi, Joel Jang, David Wadden, Noah A. Smith, Iz Beltagy, and Hannaneh Hajishirzi. Camels in a Changing Climate: Enhancing LM Adaptation with Tulu 2. *CoRR abs/2311.10702*, 2023. 6, 12
- [19] Albert Q. Jiang, Alexandre Sablayrolles, Arthur Mensch, Chris Bamford, Devendra Singh Chaplot, Diego de Las Casas, Florian Bressand, Gianna Lengyel, Guillaume Lample, Lucile Saulnier, élio Renard Lavaud, Marie-Anne Lachaux, Pierre Stock, Teven Le Scao, Thibaut Lavril, Thomas Wang, Timothée Lacroix, and William El Sayed. Mistral 7B. *CoRR abs/2310.06825*, 2023. 1, 6, 9, 12
- [20] Heng Jin, Chaoyu Zhang, Shanghao Shi, Wenjing Lou, and Y. Thomas Hou. ProFLingo: A Fingerprinting-based Copyright Protection Scheme for Large Language Models. *CoRR abs/2405.02466*, 2024. 1, 2, 3, 4, 11, 12, 15
- [21] Erik Jones, Anca D. Dragan, Aditi Raghunathan, and Jacob Steinhardt. Automatically Auditing Large Language Models via Discrete Optimization. In *International Conference on Machine Learning (ICML)*, pages 15307–15329. PMLR, 2023. 11
- [22] Peixuan Li, Pengzhou Cheng, Fangqi Li, Wei Du, Haodong Zhao, and Gongshen Liu. PLMmark: A Secure and Robust Black-Box Watermarking Framework for Pre-trained Language Models. In *AAAI Conference on Artificial Intelligence (AAAI)*, pages 14991–14999. AAAI, 2023. 1, 3
- [23] Haotian Liu, Chunyuan Li, Qingyang Wu, and Yong Jae Lee. Visual Instruction Tuning. In *Annual Conference on Neural Information Processing Systems (NeurIPS)*. NeurIPS, 2023. 9
- [24] LMSYS. Vicuna. <https://lmsys.org/blog/2023-03-30-vicuna/>. 6, 12
- [25] Hope McGovern, Rickard Stureborg, Yoshi Suhara, and Dimitris Alikaniotis. Your Large Language Models Are Leaving Fingerprints. *CoRR abs/2405.14057*, 2024. 1, 2, 3
- [26] Thomas Mesnard, Cassidy Hardin, Robert Dadashi, Surya Bhupatiraju, Shreya Pathak, Laurent Sifre, Morgane Rivière, Mihir Sanjay Kale, Juliette Love, Pouya Tafti, Léonard Hussenot, Aakanksha Chowdhery, Adam Roberts, Aditya Barua, Alex Botev, Alex Castro-Ros, Ambrose Slone, Amélie Héliou, Andrea Tacchetti, Anna Bulanova, Antonia Paterson, Beth Tsai, Bobak Shahriari, Charline Le Lan, Christopher A. Choquette-Choo, Clément Crepy, Daniel Cer, Daphne Ippolito, David Reid, Elena Buchatskaya, Eric Ni, Eric Noland, Geng Yan, George Tucker, George-Cristian Muraru, Grigory Rozhdestvenskiy, Henryk Michalewski, Ian Tenney, Ivan Grishchenko, Jacob Austin, James Keeling, Jane Labanowski, Jean-Baptiste Lespiau, Jeff Stanway, Jenny Brennan, Jeremy Chen, Johan Ferret, Justin Chiu, and et al. Gemma: Open Models Based on Gemini Research and Technology. *CoRR abs/2403.08295*, 2024. 1, 12

- [27] Meta. Llama 2 Community License. <https://ai.meta.com/llama/license/>. 2, 3
- [28] Mistral. Legal terms and conditions. <https://mistral.ai/terms/>. 2, 3
- [29] OpenAI. Chatgpt. <https://chat.openai.com/chat>. 1
- [30] OpenAI. Introducing gpts. <https://openai.com/blog/introducing-gpts>. 9
- [31] OpenAI. OpenAI API. <https://openai.com/api/>. 1
- [32] OpenAI. Terms of use. <https://openai.com/policies/row-terms-of-use/>. 2, 3
- [33] OpenAI. GPT-4 Technical Report. *CoRR abs/2303.08774*, 2023. 6, 12
- [34] OpenAI Business Licence. <https://openai.com/policies/business-terms/>. 3
- [35] Stanford. Alpaca. https://github.com/tatsu-lab/stanford_alpaca. 6
- [36] Hugo Touvron, Thibaut Lavril, Gautier Izacard, Xavier Martinet, Marie-Anne Lachaux, Timothée Lacroix, Baptiste Rozière, Naman Goyal, Eric Hambro, Faisal Azhar, Aurélien Rodriguez, Armand Joulin, Edouard Grave, and Guillaume Lample. LLaMA: Open and Efficient Foundation Language Models. *CoRR abs/2302.13971*, 2023. 1, 6, 9, 12
- [37] Hugo Touvron, Louis Martin, Kevin Stone, Peter Albert, Amjad Almahairi, Yasmine Babaei, Nikolay Bashlykov, Soumya Batra, Prajjwal Bhargava, Shruti Bhosale, Dan Bikel, Lukas Blecher, Cristian Canton-Ferrer, Moya Chen, Guillem Cucurull, David Esiobu, Jude Fernandes, Jeremy Fu, Wenyin Fu, Brian Fuller, Cynthia Gao, Vedanuj Goswami, Naman Goyal, Anthony Hartshorn, Saghar Hosseini, Rui Hou, Hakan Inan, Marcin Kardas, Viktor Kerkez, Madian Khabsa, Isabel Kloumann, Artem Korenev, Punit Singh Koura, Marie-Anne Lachaux, Thibaut Lavril, Jenya Lee, Diana Liskovich, Yinghai Lu, Yuning Mao, Xavier Martinet, Todor Mihaylov, Pushkar Mishra, Igor Molybog, Yixin Nie, Andrew Poulton, Jeremy Reizenstein, Rashi Rungta, Kalyan Saladi, Alan Schelten, Ruan Silva, Eric Michael Smith, Ranjan Subramanian, Xiaoqing Ellen Tan, Binh Tang, Ross Taylor, Adina Williams, Jian Xiang Kuan, Puxin Xu, Zheng Yan, Iliyan Zarov, Yuchen Zhang, Angela Fan, Melanie Kambadur, Sharan Narang, Aurélien Rodriguez, Robert Stojnic, Sergey Edunov, and Thomas Scialom. Llama 2: Open Foundation and Fine-Tuned Chat Models. *CoRR abs/2307.09288*, 2023. 6, 12
- [38] Weihang Wang, Qingsong Lv, Wenmeng Yu, Wenyi Hong, Ji Qi, Yan Wang, Junhui Ji, Zhuoyi Yang, Lei Zhao, Xixuan Song, Jiazheng Xu, Bin Xu, Juanzi Li, Yuxiao Dong, Ming Ding, and Jie Tang. CogVLM: Visual Expert for Pretrained Language Models. *CoRR abs/2311.03079*, 2023. 9
- [39] Jiashu Xu, Fei Wang, Mingyu Derek Ma, Pang Wei Koh, Chaowei Xiao, and Muhao Chen. Instructional Fingerprinting of Large Language Models. *CoRR abs/2401.12255*, 2024. 1, 3, 6, 15
- [40] Ziqing Yang, Michael Backes, Yang Zhang, and Ahmed Salem. SOS! Soft Prompt Attack Against Open-Source Large Language Models. *CoRR abs/2407.03160*, 2024. 1, 3
- [41] Yuan Yao, Tianyu Yu, Ao Zhang, Chongyi Wang, Junbo Cui, Hongji Zhu, Tianchi Cai, Haoyu Li, Weilin Zhao, Zhihui He, Qianyu Chen, Huarong Zhou, Zhen-sheng Zou, Haoye Zhang, Shengding Hu, Zhi Zheng, Jie Zhou, Jie Cai, Xu Han, Guoyang Zeng, Dahai Li, Zhiyuan Liu, and Maosong Sun. MiniCPM-V: A GPT-4V Level MLLM on Your Phone. *CoRR abs/2408.01800*, 2024. 9
- [42] Rowan Zellers, Ari Holtzman, Yonatan Bisk, Ali Farhadi, and Yejin Choi. HellaSwag: Can a Machine Really Finish Your Sentence? In *Annual Meeting of the Association for Computational Linguistics (ACL)*, pages 4791–4800. ACL, 2019. 6
- [43] Boyi Zeng, Chenghu Zhou, Xinbing Wang, and Zhouhan Lin. HuRef: HUMAN-READABLE Fingerprint for Large Language Models. *CoRR abs/2312.04828*, 2023. 1, 2, 3, 15
- [44] Lianmin Zheng, Wei-Lin Chiang, Ying Sheng, Siyuan Zhuang, Zhanghao Wu, Yonghao Zhuang, Zi Lin, Zhuohan Li, Dacheng Li, Eric P. Xing, Hao Zhang, Joseph E. Gonzalez, and Ion Stoica. Judging LLM-as-a-Judge with MT-Bench and Chatbot Arena. In *Annual Conference on Neural Information Processing Systems (NeurIPS)*. NeurIPS, 2023. 12
- [45] Andy Zou, Zifan Wang, J. Zico Kolter, and Matt Fredrikson. Universal and Transferable Adversarial Attacks on Aligned Language Models. *CoRR abs/2307.15043*, 2023. 11, 12, 14

A Existing Passive Identification Methods

In this section, we measure the effectiveness of current passive identification methods. We mainly consider the state-of-the-art black-box LLM identification methods that are based on adversarial examples (AE) [10, 15, 21, 45]. We experiment on four base LLMs, along with 30 LLMs and two real-world black-box APIs as suspect models to measure their effectiveness and reliability in identifying the origin of an LLM.

A.1 AE-Based Identification Methods

AE-based methods [14, 20] primarily optimize an adversarial text for the base model, which can serve as a prefix/suffix to the input query to generate specific outputs. Specifically, adversarial examples are optimized for generating specific outputs based on some input queries. To determine whether the suspect model is derived from the base model, they analyze the responses of the suspect model to the queries with AEs. They consider a suspect model as probably derived

Table 7: Performance of TRAP. Cells highlighted in red signify that the suspect model is derived from the base model and is expected to exhibit a higher TRR. Unhighlighted cells correspond to non-derivative models, expecting to achieve a lower TRR.

Suspect Model	Base Model			
	llama-7b	Llama-2-7b	Mistral-7B-v0.1	gemma-7b
yahma/llama-7b-hf	1.00	0.00	0.00	0.00
lmsys/vicuna-7b-v1.3	0.00	0.00	0.00	0.00
meta-llama/Llama-2-7b-hf	0.00	0.95	0.00	0.00
meta-llama/Llama-2-7b-chat-hf	0.00	0.00	0.00	0.00
mistralai/Mistral-7B-v0.1	0.00	0.00	1.00	0.00
mistralai/Mistral-7B-Instruct-v0.1	0.00	0.00	0.00	0.00
google/gemma-7b	0.00	0.00	0.00	0.96
google/gemma-7b-it	0.00	0.00	0.00	0.00
gpt-4-turbo-2024-04-09	0.00	0.00	0.00	0.00
claude-3-5-sonnet-20240620	0.00	0.00	0.00	0.00

from the base model if the responses are similar to the target outputs. Such methods do not require modifying the base model before its distribution, so we categorize these methods as passive identification.

TRAP. TRAP [14] optimizes an adversarial text suffix for the target base model to generate a target string of digits based on GCG [45]. Then, it uses the suffix to query the black-box API and compare the output with the target string. A match indicates that the target base model may power the black-box LLM.

ProFlingo. ProFlingo [20] utilizes a similar optimization process to obtain an adversarial text prefix. Compared to TRAP, ProFlingo optimizes several prompt templates simultaneously and accelerates the prefix optimization process. Furthermore, the query set used by ProFlingo differs. ProFlingo queries with standard questions and expects absurd responses. For example, with the query “Where does the sun rise?” ProFlingo optimizes an adversarial example, causing the LLM to answer “North.”

A.2 Experimental Settings

Models. We utilize four *base models*, including llama-7b [36], Llama-2-7b [37], Mistral-7B-v0.1 [19], and gemma-7b [26]. We have white-box access to them and aim to identify whether they are the origin of the suspect black-box LLM. Then, we collect extensive models as *suspect models* for evaluation, including 30 open-source LLMs and two real-world black-box APIs. Specifically, some models derived from the base models are released officially, e.g., Llama-2-7b-chat [37] developed by Meta. Some are released by other institutes, e.g., vicuna-7b-v1.3 [24] (fine-tuned on llama-7b) from LMSYS Org and tulu-2-7b [18] (fine-tuned on Llama-2-7b) from AllenAI. We also collect other model families, such as OLMo [12]. As for the two black-box APIs, we collect gpt-4-turbo-2024-04-09 [33] and claude-3-5-sonnet-20240620 [2] as suspect models for evaluation.

Investigation Setup. We follow the default settings in TRAP and ProFlingo for AE optimization. We use the top-p of 1.0 and temperature of 1.0 as default settings when generating

responses. In evaluation, we use the prompt template suggested in its repository for each model if available. Otherwise, we default to the zero-shot prompt template from FastChat [44].

Evaluation Metric. We use the target response rate (TRR) as our evaluation metric, which measures the ratio of the number of queries that the suspect model outputs the target output over the number of all queries. A higher TRR indicates a higher probability that the suspect model is derived from the base model.

Note. Note that we directly employ the learned adversarial text prefix of Llama-2-7b and Mistral-7B-v0.1 released by ProFlingo to conduct the evaluation.

A.3 Experimental Results

TRAP. Table 7 presents the primary experimental results for TRAP, which show the TRRs of various suspect models based on our four different base LLMs. We only show the representative results here, as the results for other suspect models are nearly zero. Specifically, for each base model, we report their results on two black-box APIs and the other two suspect models, including the base model itself and its official fine-tuned version. As llama-7b does not have an official fine-tuned version, we choose lmsys/vicuna-7b-v1.3 [24] as its fine-tuned version. We observe that TRAP consistently achieves a high TRR on identical models, e.g., the base Mistral-7B-v0.1 achieves a TRR of 1.00 on the suspect mistralai/Mistral-7B-v0.1. Conversely, it records nearly zero TRRs for dissimilar models, even for the base model’s official instruction-tuned version, i.e., released by Mistral AI as well. This includes mistralai/Mistral-7B-Instruct-v0.1 and other unrelated suspect models. This suggests that TRAP works well with identical models under a similar setting when the parameters remain unchanged. However, it fails to distinguish the relationship between the base model and its derivatives when the derivative is further fine-tuned.

ProFlingo. Table 8 exhibits ProFlingo’s performance of identifying multiple suspect models on our four base models. We observe that, compared with TRAP, ProFlingo

Table 8: Performance of ProFlingo. Cells highlighted in red signify that the suspect model is derived from the base model. The lowest TRR observed among the derivatives of the base model is underlined. In unhighlighted cells, results are bolded if the TRR is not below this underlined TRR. Bolded results in these cells likely suggest a misidentification of the relationship between the suspect and the base model.

Suspect Model	Base Model			
	llama-7b	Llama-2-7b	Mistral-7B-v0.1	gemma-7b
yahma/llama-7b-hf	0.96	0.10	0.04	0.02
lmsys/vicuna-7b-v1.3	0.56	0.04	0.02	0.04
TheBloke/guanaco-7B-HF	<u>0.14</u>	0.00	0.00	0.04
meta-llama/Llama-2-7b-hf	0.02	1.00	0.04	0.00
meta-llama/Llama-2-7b-chat-hf	0.06	<u>0.04</u>	0.02	0.06
lmsys/vicuna-7b-v1.5	0.12	0.58	0.02	0.06
codellama/CodeLlama-7b-hf	0.14	0.12	0.14	0.08
codellama/CodeLlama-7b-Python-hf	0.14	0.20	0.12	0.08
codellama/CodeLlama-7b-Instruct-hf	0.10	0.14	0.06	0.02
allenai/tulu-2-7b	0.02	0.28	0.00	0.00
allenai/tulu-2-dpo-7b	0.00	0.18	0.00	0.02
allenai/scitulu-7b	0.04	0.34	0.02	0.02
microsoft/Orca-2-7b	0.06	0.38	0.04	0.08
georgesung/llama2_7b_chat_uncensored	0.08	0.50	0.02	0.08
mistralai/Mistral-7B-v0.1	0.00	0.00	1.00	0.00
mistralai/Mistral-7B-Instruct-v0.1	0.04	0.04	0.14	0.02
HuggingFaceH4/zephyr-7b-beta	0.10	0.10	<u>0.12</u>	0.06
mistralai/Mistral-7B-v0.3	0.04	0.02	0.74	0.02
mistralai/Mistral-7B-Instruct-v0.3	0.20	0.18	0.42	0.12
google/gemma-7b	0.12	0.04	0.04	0.90
google/gemma-7b-it	0.00	0.04	0.02	0.10
HuggingFaceH4/zephyr-7b-gemma-v0.1	0.06	0.02	0.02	<u>0.06</u>
HuggingFaceH4/zephyr-7b-gemma-sft-v0.1	0.04	0.08	0.12	0.12
openlm-research/open_llama_7b	0.08	0.12	0.02	0.02
openlm-research/open_llama_7b_v2	0.08	0.10	0.06	0.08
meta-llama/Meta-Llama-3-8B	0.00	0.04	0.02	0.06
meta-llama/Meta-Llama-3-8B-Instruct	0.02	0.00	0.02	0.04
allenai/OLMo-7B-hf	0.04	0.06	0.02	0.02
allenai/OLMo-7B-SFT-hf	0.02	0.04	0.04	0.10
allenai/OLMo-7B-Instruct-hf	0.02	0.08	0.06	0.12
gpt-4-turbo-2024-04-09	0.00	0.00	0.00	0.00
claude-3-5-sonnet-20240620	0.00	0.00	0.00	0.00

shows more generalizability to the derivatives, i.e., models derived from or related to the base model. For example, with Llama-2-7b as the base model, ProFlingo successfully achieves a TRR of 1.00 on the suspect meta-llama/Llama-2-7b-hf and 0.58 on lmsys/vicuna-7b-v1.3. It also achieves a zero TRR for both gpt-4-turbo-2024-04-09 and claude-3-5-sonnet-20240620, indicating that the LLMs powering the services are not derivatives of Llama-2-7b. However, there are many counterexamples that prove ProFlingo is unreliable in certain situations. Take Llama-2-7b as the base model as well. ProFlingo only achieves a TRR of 0.04 on the suspect meta-llama/Llama-2-7b-chat-hf, the official instruct-tuned version of itself, which is even lower than that on the suspect llama-7b (TRR of 0.10) and the suspect allenai/OLMo-7B-Instruct-hf (TRR of 0.08). With the base gamma-7b,

Table 9: Time (GPU hours) used for adopting existing AE-based identification methods on llama-7b.

	Time Per Sample	Total Time
TRAP	1.56	156.0
ProFlingo	0.51	25.5

ProFlingo attains a TRR of 0.10 on google/gemma-7b-it while achieving a TRR of 0.12 on mistralai/Mistral-7B-Instruct-v0.3 and allenai/OLMo-7B-Instruct-hf. This suggests that while ProFlingo can distinguish more derivatives of the base model, it is *not* reliable enough to identify the model’s origin in some circumstances.

Efficiency. We compare the efficiency of both methods. Table 9 shows the GPU hour cost of each method’s optimization process. In the experiment, we use NVIDIA A100 GPUs with 40 GB of memory. The results show that both methods cost over 24 GPU hours for optimization. TRAP even requires 156 GPU hours, which is six times longer than ProFlingo. Note that we only experimented with 7B models; it would be more time-consuming for larger models in practice. This suggests that a more efficient method is needed.

Threshold Determination. We further examine the strategies used to determine whether a suspect model relates to the base model in both methods. TRAP measures the identification success using the true positive rate. However, it did not provide a strategy for selecting a threshold to distinguish between related and unrelated suspect models based on their results. Instead, ProFlingo claims that they infer that the suspect model is derived from the base model if its TRR is significantly higher compared to the TRRs of other models that are not derivatives. In other words, they empirically set the threshold as the highest TRR on other unrelated models. There is no valid theoretical analysis or proof to support this. They also fail to claim how to obtain the set of unrelated models. Further, the bolded cells in Table 8 have already shown several counterexamples that the TRRs of non-derivative models are higher than the base model’s derivatives. This suggests that the strategy for determination also needs to be further improved.

Summary. Our findings indicate that TRAP is limited in its ability to identify derivatives of a base model, as it can only recognize the base model itself. In contrast, ProFlingo demonstrates better efficacy compared to TRAP in detecting derivatives of LLMs. Yet, ProFlingo still misclassifies derivatives and non-derivatives in a noticeable number of cases. We show that both methods cannot deterministically assess whether a suspect model is a derivative of the base model. Instead, they provide a result of TRR that reflects the suspect model’s possibility to be derivative and subsequently rely upon an empirical threshold to make a verdict.

A.4 Why Are They Falling Flat?

To understand why these AE-based passive identification methods become unreliable against fine-tuning, we formalize both TRAP and ProFlingo under a unified loss function. This allows us to conduct a comprehensive investigation of their inherent limitations.

TRAP. TRAP is based on GCG [45]. Its objective is to optimize an adversarial suffix, denoted as a , that manipulates the reference model into producing a predetermined target response y^* , given the input query x . TRAP’s loss function can be formulated as follows:

$$\begin{aligned} \mathcal{L}_{\text{TRAP}}(y^*, x, a) &= \mathcal{L}(\text{encode}(y^*), \text{encode}(h(x||a))) \\ &= \mathcal{L}(t^{y^*}, t^{h(x||a)}), \end{aligned} \quad (9)$$

where $h \in H$ represents the base model’s prompt template, and $||$ denotes the concatenation between texts. t^{y^*} and $t^{h(x||a)}$ represent the encoded token sequence of y^* and $h(x||a)$, accordingly. Then, TRAP optimizes the adversarial suffix a to

minimize this loss function by iteratively comparing the loss value and replacing the tokens in the suffix.

ProFlingo. ProFlingo improves TRAP in four aspects. First, ProFlingo uses a different query set. Second, ProFlingo’s optimization objective is an adversarial prefix instead of a suffix. Third, instead of using only a single prompt template, ProFlingo optimizes several templates simultaneously to improve the algorithm’s robustness. Furthermore, ProFlingo proposes a new way to update the adversarial prefix, which enhances the process of generating adversarial examples and the efficiency of the overall algorithm. ProFlingo’s loss function is formulated as follows:

$$\begin{aligned} \mathcal{L}_{\text{ProFlingo}}(y^*, x, a) &= \sum_{h \in H} \mathcal{L}(\text{encode}(y^*), \text{encode}(h(a||x))) \\ &= \sum_{h \in H} \mathcal{L}(t^{y^*}, t^{h(a||x)}), \end{aligned} \quad (10)$$

where H is a collection of prompt templates that can be manually designed. The adversarial prefix a is optimized to minimize its loss function.

Unified Loss. Based on Equation 9 and Equation 10, we present a unified loss function summarizing the above AE-based identification methods:

$$\mathcal{L}_{\text{AE}}(y^*, x, a) = \sum_{h \in H} \mathcal{L}(t^{y^*}, I(t^{h(x)}, t^a, z_h)), \quad (11)$$

where $I(t^{h(x)}, t^a, z_h)$ denotes the insertion of the token sequence t^a into the token sequence $t^{h(x)}$ of the input x , at the position specified by z_h . It is important to note that the position z_h is adaptable, enabling support for various prompt templates. For instance, the unified loss \mathcal{L}_{AE} can be translated into $\mathcal{L}_{\text{ProFlingo}}$ if we insert the adversarial example a as input x ’s prefix, i.e., let $I(t^{h(x)}, t^a, z_h) := t^{h(a||x)}, \forall h \in H$. It is also noteworthy that the insertion operation $I(\cdot, \cdot, \cdot)$ can be applied not only to token sequences but also to embedding sequences, thereby extending its applicability across different levels of representation.

Limitations of TRAP and ProFlingo. We compare TRAP and ProFlingo under the unified loss \mathcal{L}_{AE} . As discussed above, the unified loss can be translated into the $\mathcal{L}_{\text{ProFlingo}}$ loss function when $I(t^{h(x)}, t^a, z_h) := t^{h(a||x)}$. Likewise, this unified loss can be adapted to $\mathcal{L}_{\text{TRAP}}$ by defining the prompt template collection as $H = \{h\}$, where h represents the default template of the base model, and appending a after x , i.e., setting $I(t^{h(x)}, t^a, z_h) := t^{h(x||a)}$. We find $\mathcal{L}_{\text{TRAP}}$ is more restricted as it optimizes to only one prompt template, while $\mathcal{L}_{\text{ProFlingo}}$ optimizes several prompt templates simultaneously (see Equation 10), which allows a more generalizable adversarial text that is resilient to larger disturbances. This could explain why TRAP can only identify the base model itself, while ProFlingo can identify more derivatives of the base model, as shown in Appendix A.3.

Recall that we focus on the task of black-box LLM identification, where interaction with the target model is restricted to text inputs. The defender optimizes an adversarial prefix/suffix to query the suspect model. However, because text

is composed of discrete tokens, the optimization process inherently operates in a discrete space. For example, ProFlingo first calculates the gradient for each token t_i^a in the prefix a in each epoch as $\nabla_{t_i^a} \mathcal{L}_{\text{AE}}$. As we can only replace t_i^a instead of optimizing it directly, ProFlingo updates the adversarial prefix by replacing multiple tokens in each epoch. Based on the top- k tokens with the most negative gradients, a set of candidate tokens for replacement is sampled. Subsequently, the loss associated with each potential replacement token is computed. The token with the minimal loss is then selected. TRAP follows a similar process, optimizing over a discrete set of inputs. However, such discrete optimization approaches present significant challenges. Given the limited number of tokens and the computationally intensive nature of the optimization process, it is difficult to achieve a local optimum by design.

B Challenges

Our comprehensive experiments on various methods have illustrated the difficulties of identifying the origin of a black-box LLM. Drawing from theoretical and empirical analysis in this study, we highlight the challenges and opportunities.

The first challenge is that the auditor may not have sufficient knowledge of practical customizations applied to LLMs. For example, the LLM may be further fine-tuned with specific system prompts and equipped with specific hyperparameters [14, 20]. The model’s structure and weight can also be modified or rearranged [43]. For example, existing methods and PlugAE are proven ineffective for models that adopt the Llama architecture yet are trained independently (e.g., openlm-research/open_llama_7b).

The second challenge is the black-box access to the suspect model. It implies that we can only query the model with texts and obtain the text response. This is inevitable as the malicious third party tends to conceal the model’s true origin. Such black-box access inevitably limits the identification methods as they are constrained to querying the model and analyzing the text outputs. For example, existing AE-based methods rely on discrete optimization, as they cannot directly query the LLM with embeddings but with discrete texts. As analyzed in Section 4.1, such discrete optimization is hard to reach optimal, leading to performance degradation. Additionally, the adapter variant of Instructional Fingerprint [39] is not applicable as we are unable to insert an F-Adapter to the black-box LLM. Our experimental results show that PlugAE surpasses existing methods, though its efficacy declines when substantial weight modifications are present.